

To Buffer or Not To Buffer: IEEE 802.11p/bd Performance Under Different Buffering Strategies

Andrea Baiocchi*, Ion Turcanu[†] and Alexey Vinel[‡]

*Dept. of Information Engineering, Electronics and Telecommunications (DIET), University of Rome Sapienza, Italy

[†]Interdisciplinary Centre for Security, Reliability and Trust (SnT), University of Luxembourg

[‡]School of Information Technology, Halmstad University, Sweden

andrea.baiocchi@uniroma1.it, ion.turcanu@uni.lu, alexey.vinel@hh.se

Abstract—A fundamental paradigm of the Internet of Things (IoT) consists of agents that communicate updates to each other to perform joint actions, e.g., cooperative awareness in transportation systems, swarms of Unmanned Aerial Vehicles (UAVs), fleet of robots, automated assembly lines and logistics. A common feature of update messaging is emphasis on reliable throughput and freshness of collected data. We develop an analytical model that yields accurate predictions of all relevant metrics, both in terms of moments and probability distributions, for the case of one-hop broadcast update messages exchanged by using a CSMA-based wireless network. The model is validated against simulations and then applied to compare two update message scheduling approaches: providing a minimal buffer resource or providing no buffer. Surprisingly, we prove that having no buffer improves Age of Information (AoI) performance as well as message delivery rate, in spite of dropped packets. This is essentially due to much smaller congestion and hence collision probability in the wireless channel. From a system point of view this suggests a simple design of message handling, with no need of buffering and overwriting older messages. From a modeling point of view, the result supports the definition of simpler models that need not keep into account buffer state.

Index Terms—Age of Information, MAC Access Delay, IEEE 802.11p/bd, CSMA Networks, Vehicular Networks, Message Buffering Policies.

I. INTRODUCTION

The expected spread of smart infrastructures relies consistently on highly flexible and performing communication networks. Smart environments often encompass agents interacting by message exchanges. Distributed control processes leverage on state updates that are repeatedly issued towards each node's neighbors. Examples of such environments can be found in Cooperative Intelligent Transportation Systems (C-ITS), where cooperative driving and autonomous vehicles rely on high-frequency beacon message exchange. A specific example of vehicle coordination that poses strict timeliness and reliability requirements is platooning, where a fleet of coordinated vehicles travel in tight formation [1]. Swarms of aerial vehicles that move in a coordinated way, e.g., in rescue operations, surveillance, exploration and many other missions, require tight cooperation among nodes [2]. Other notable examples can be found in industrial processes automation, where teams of robots and moving machines cooperate in assembly lines. Navigation safety messaging among robots is investigated, e.g., in [3]. Also, logistics is increasingly automated and realized by moving robots in large storage

plants [4]. Communications in all these cases are supported via radio channels, using technologies from the so called proximity networks exploited in the Internet of Things (IoT).

In this work, we focus on Carrier-Sense Multiple Access (CSMA) networks, e.g., as used in Wi-Fi and, specifically, in the amendment devised for vehicular applications, namely IEEE 802.11p [5] and its evolution IEEE 802.11bd [6]. The model we develop is applicable to CSMA networks fed by one-hop broadcast traffic, typical of updates in the context mentioned above. We aim at providing:

- an accurate and efficient analytical model to predict critical performance metrics, e.g., reliability, delay, age of information;
- closed-form equations to evaluate several performance metrics, including the age of information, both the mean value and the tail of the Probability Density Function (PDF) (quantiles);
- insight into dependencies and impact of key system parameters and guidelines on system design, specifically, scheduling and buffering alternatives at nodes.

The research on analytical modeling of IEEE 802.11 CSMA networks has been for many years inspired by the seminal papers [7] and [8], where networks in saturation mode are considered and throughput – being the main performance metric for Wi-Fi networks – is analyzed. Characterization of the respective queuing delay for an arbitrary offered load turns out to be a challenging problem and was performed, for example, in [9].

With the rise of IoT, the analysis of beaconing in IEEE 802.11p, i.e. broadcasting of updates, became of interest. It, in some sense, represents an easier case with respect to traditional Wi-Fi unicasting since the lack of retransmissions imposes no increase of contention window, which simplifies the analysis of the CSMA backoff technique [10]. At the same time, the need for coupling of wireless communications and networked control motivated the design of freshness-related metrics resulted in the formulation of the Age of Information (AoI) metric [11] and applying it to the CSMA environment [12]–[14].

Naturally, the traditional FIFO queuing service discipline with standard buffer, which lets newly arrived packets wait while outdated ones are served, is unattractive for the beaconing use case. Eenennaam et al. [15] demonstrate that the oldest

packet drop policy can significantly improve the freshness of the received beacons in close to saturation conditions.

There is surprisingly relatively little literature dedicated to the buffer sizing in 802.11 networks, although it might severely impact both network utilization and queuing delays [16]. In the context of the IEEE 802.11p/bd AoI, this problem becomes even more prominent because it is desirable that newly arrived packets overwrite older ones, so that small buffer or no-buffering at all seems to be a natural approach. In [17] it is also argued that buffer sizes larger than five are not needed with oldest packet drop policy.

In this work we look further into the tradeoff between a very small buffer size, i.e. one packet maximum and no buffering at all, in IEEE 802.11p/bd MAC layer from the AoI perspective. The analytical model is provided for both cases. The main point is that in the former case one reduces the chance of the node to be idle, while in contradiction to intuition, the latter case turns out to be preferable both from the AoI and throughput points of view.

The rest of the paper is organized as follows. Section II introduces the model, including assumptions and the two scheduling approaches considered in the following. Section III presents the mathematical development of model analysis. The model is validated against simulations in Section IV and used to investigate and compare the two message scheduling policies considered in this work in Section V. Finally, conclusions are drawn in Section VI.

II. SYSTEM MODEL

We consider a network composed of n nodes that support cooperative applications requiring continuous exchange of broadcast messages. We assume that all nodes are within range of one another. The time axis is divided into *virtual time slots*, i.e., the time intervals elapsing between two successive idle back-off time slots.

We assume that new messages are generated at each node according to a Poisson process with mean rate λ . New messages are generated at upper layer and passed down to the MAC layer entity for immediate transmission. Once a node MAC entity is engaged with contention/transmission of a message, it cannot be interrupted. Further arriving messages, if any, must wait for the current contention/transmission operation to terminate or be dropped.

We assume that the radio access of the vehicular network is based on IEEE 802.11bd [6]. Physical layer parameters are set as in [18].

We aim at devising a model to predict delay and AoI performance of the vehicular network under cooperative application update message traffic. We then use the model to compare two message handling strategies at MAC layer:

- 1) Last Come First Served with Overwrite (LCFSwO): if the node is engaged in contention/transmission of a previous message, a new arriving message is stored in a one-packet buffer. The latest arriving message overwrites whatever is already stored in the buffer.

- 2) No Buffering (NoB): if the node is engaged in contention/transmission of a previous message, a new arriving message is dropped. No buffer is provided at MAC layer.

It is to be stressed that message handling strategies listed here refer to cooperative awareness applications, that are based on regularly issued updates. For those applications, only the latest update is relevant. It is shown in [15] that dropping older messages is beneficial to delay. We will see that the NoB policy improves even further both access delay and AoI in the considered use case. This applies not only to mean values but also to tails of probability distributions.

The model is obtained by considering the point of view of a tagged node, say node i . We drop the subscript denoting the tagged node, unless required to avoid ambiguity. If not stated explicitly, it is understood that each variable or quantity refers to the tagged node.

III. MODEL ANALYSIS

Let t_k denote the time when the transmission of a packet of the tagged node is completed (k -th departing packet). We write $Q_k = Q(t_k+)$ to denote the queue length left behind by the k -th departing packet. With LCFSwO policy, the queue status of the tagged node can be either 0 (empty queue) or 1, in case there is a packet ready. In case of NoB policy, the queue status is constantly equal to 0.

A. Virtual slot time

Virtual slot times can be distinguished according to whether the tagged node does or does not transmit. In the following we refer only to the latter kind of virtual slot times, i.e., those when the tagged node is either idle or counting down its back-off counter. The virtual time slot duration is denoted with X .

We denote the transmission time with T_0 . It includes any overhead implied by the MAC protocol operations (preamble, headers and AIFS). Moreover, let δ denote the back-off slot time. Then, the virtual slot time seen by the tagged node is given by

$$X = \begin{cases} \delta & \text{w.p. } q \\ \delta + T_0 & \text{w.p. } 1 - q. \end{cases} \quad (1)$$

where q is the probability that no other node transmits in a virtual slot time. Let τ be the probability that a node transmits in a virtual slot time. Then

$$q = (1 - \tau)^{n-1} \quad (2)$$

We will see in Section III-F that τ is computed by means of a fixed point equation.

The Laplace transform of the PDFs of X is given by

$$\varphi_X(s) = qe^{-\delta s} + (1 - q)e^{-(T_0+\delta)s} \quad (3)$$

B. Inter-departure time

Let Y_k denote the inter-departure time between packet $k-1$ and k , i.e., $Y_k = t_k - t_{k-1}$. Let also C_k denote the service time of the k -th departing packet, defined as the time elapsing since the first idle back-off slot of the count down occurs until the packet transmission is completed (including the ensuing

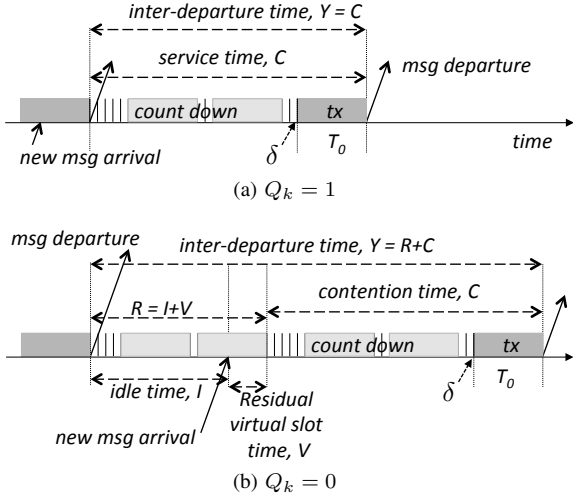


Figure 1. Time evolution of the channel and definition of main time intervals of the node model.

AIFS required for any other action on the wireless channel to be taken by any node).

We can distinguish two situations (see Figure 1). If there is already a packet ready to go upon the departure of the k -th packet, i.e., if $Q_k = 1$, contention starts immediately after packet departure. Therefore the time for the next packet to leave equals a service time C_{k+1} , i.e., $Y_{k+1} = C_{k+1}$ (time diagram in Figure 1a). If instead the k -th departing packet leaves behind an empty queue, the node stays idle until next packet arrives (idle time I_{k+1} ; see the time diagram of Figure 1b). In the meantime, the wireless channel is used by nodes other than the tagged one. The packet starting a new busy period has to wait for a residual virtual time slot, denoted with V_{k+1} . Then its contention starts. Overall, the inter-departure time is $Y_{k+1} = I_{k+1} + V_{k+1} + C_{k+1}$. In the following we denote $R_{k+1} = I_{k+1} + V_{k+1}$.

Summing up, we have

$$Y_{k+1} = \begin{cases} C_{k+1} & \text{if } Q_k = 1, \\ R_{k+1} + C_{k+1} & \text{if } Q_k = 0. \end{cases} \quad (4)$$

Given Equation (4), we find:

$$\varphi_Y(s) = \pi_0 \varphi_R(s) \varphi_C(s) + (1 - \pi_0) \varphi_C(s) \quad (5)$$

where $\pi_0 = \mathcal{P}(Q = 0)$. An expression for π_0 is given in Equation (11). The PDFs of C and R are studied in Section III-C and Section III-D, respectively.

C. Service time

The tagged node decrements its back-off counter by one for each idle back-off time slot it sees on the channel. If we denote the initial counter level with K , the service time C consists of $K - 1$ virtual time slots and a final transmission time slot,

where the tagged node transmits, possibly along with other nodes (collision). Therefore, we have

$$C = \sum_{j=1}^K X^{(j)} + \delta + T_0 \quad (6)$$

where K is a discrete random variable uniformly distributed in the set $\{1, \dots, W_0\}$, and W_0 is the size of the contention window.

The Laplace transform of the PDF of C is:

$$\varphi_C(s) = e^{-s(\delta+T_0)} \frac{1 - \varphi_X(s)^{W_0}}{W_0[1 - \varphi_X(s)]}. \quad (7)$$

D. Idle time

The time elapsed from the departure of a packet that leaves an empty queue behind and the beginning of the contention time of the next arriving packet, namely R , is the sum of N consecutive virtual time slots:

$$R = \sum_{i=1}^N X^{(i)} \quad (8)$$

where N is a discrete random variable, defined as the number of virtual slots until a new packet arrives at the tagged node.

From the definition in Equation (8), conditional on $N = h$ and on $X^{(j)} = x_j$, $j = 1, \dots, h$, it is $R = x_1 + \dots, x_h$. Hence

$$\mathbb{E}[e^{-sR} | N = h, X^{(1)} = x_1, \dots, X^{(h)} = x_h] = \prod_{j=1}^h e^{-sx_j}.$$

Since arrivals occur according to a Poisson process of mean rate λ , the probability of $N = h$, conditional on $X^{(j)} = x_j$, $j = 1, \dots, h$, is $e^{-\lambda x_1} \dots e^{-\lambda x_{h-1}} (1 - e^{-\lambda x_h})$. Removing the conditioning we have:

$$\begin{aligned} \varphi_R(s) &= \sum_{h=1}^{\infty} \int_0^{\infty} (1 - e^{-\lambda x_h}) f_X(x_h) e^{-sx_h} dx_h \\ &\quad \times \prod_{j=1}^{h-1} \int_0^{\infty} e^{-\lambda x_j} f_X(x_j) e^{-sx_j} dx_j \\ &= \sum_{h=1}^{\infty} [\varphi_X(s + \lambda)]^{h-1} [\varphi_X(s) - \varphi_X(s + \lambda)] \\ &= \frac{\varphi_X(s) - \varphi_X(s + \lambda)}{1 - \varphi_X(s + \lambda)}. \end{aligned} \quad (9)$$

Let us now turn to the evaluation of the Laplace transform of the PDF of V . It is the time elapsing since the *last* arrival within a virtual time slot and the end of that virtual time slot. The Laplace transform of the PDF of V is found in the Appendix, Equation (33). It is:

$$\varphi_V(s) = \frac{\lambda}{1 - \varphi_X(\lambda)} \frac{1 - \varphi_X(s + \lambda)}{s + \lambda} \quad (10)$$

E. Probability of empty queue

Let $\pi_0 = \mathcal{P}(Q = 0)$ and $\pi_1 = \mathcal{P}(Q = 1)$. These probabilities can be found by using the transition probabilities between the two states $Q = 1$ and $Q = 0$, namely

$$\begin{aligned} p_{10} &\equiv \mathcal{P}(Q_{k+1} = 0 | Q_k = 1) \\ &= \mathcal{P}(\text{no arrival in } C_{k+1}) = \varphi_C(\lambda) \\ p_{00} &\equiv \mathcal{P}(Q_{k+1} = 0 | Q_k = 0) \\ &= \mathcal{P}(\text{no arrival in } V_{k+1} + C_{k+1}) = \varphi_V(\lambda)\varphi_C(\lambda) \end{aligned}$$

Using the equations above, the balance equations $\pi_0 = \pi_0 p_{00} + \pi_1 p_{10}$ and $\pi_0 + \pi_1 = 1$, we find

$$\pi_0 = \frac{\varphi_C(\lambda)}{1 + \varphi_C(\lambda) - \varphi_C(\lambda)\varphi_V(\lambda)} \quad (11)$$

Note that $\varphi_V(\lambda) = -\lambda\varphi'(\lambda)/[1 - \varphi_X(\lambda)]$.

F. Probability of transmission

In order to find τ , we use the renewal reward theorem. Let M be the number of virtual slots between two successive transmissions of the tagged node. We have then $\tau = 1/\mathbb{E}[M]$. Let us consider two consecutive packets departing from the tagged node, say $P1$ and $P2$. If the tagged node is idle upon arrival of $P2$, it is $M = N + K$ (for the definitions of N and K see Equations (6) and (8)). If instead $P2$ is already available at the tagged node when $P1$ departs, it is $M = K$.

It is easy to check that N has a geometric probability distribution:

$$\mathcal{P}(N = h) = [1 - \varphi_X(\lambda)] \varphi_X(\lambda)^{h-1}, \quad h \geq 1. \quad (12)$$

while K has a uniform probability distribution between 1 and W_0 . The mean of M is therefore

$$\begin{aligned} \mathbb{E}[M] &= \pi_0 (\mathbb{E}[N] + \mathbb{E}[K]) + (1 - \pi_0)\mathbb{E}[K] \\ &= \pi_0 \frac{1}{1 - \varphi_X(\lambda)} + \frac{W_0 + 1}{2} \end{aligned} \quad (13)$$

We have finally:

$$\tau = \frac{1}{\mathbb{E}[M]} = \frac{1}{\frac{W_0+1}{2} + \frac{\pi_0}{1-\varphi_X(\lambda)}} = \frac{\tau_0}{1 + \tau_0 \frac{\pi_0}{1-\varphi_X(\lambda)}} \quad (14)$$

where $\tau_0 = 2/(W_0 + 1)$ is the probability of transmission in a virtual slot in saturation. It can be checked that $\tau \rightarrow 0$ as $\lambda \rightarrow 0$ (light traffic regime), while $\tau \rightarrow \tau_0$ for $\lambda \rightarrow \infty$ (heavy traffic regime).

The transmission probability τ is a function of π_0 and $\varphi_X(\lambda)$, both of which depend upon q , which in turn depends on τ . Hence τ is computed by solving Equation (14) as a fixed point equation $\tau = F(\tau)$. Since $F(\cdot)$ defines a continuous map of the interval $[0, 1]$ onto itself, we can appeal to Brouwer's theorem to guarantee that the fixed point iteration converges.

G. Successful delivery probability and throughput

The probability γ of a successful reception, conditional on a transmission attempt, is

$$\gamma = (1 - \tau)^{n-1} (1 - \text{PER}) \quad (15)$$

where PER is the packet error ratio, i.e., the fraction of packets that are detected with errors, given that no collision occurred. In deriving γ , we assume that collision and successful packet detection are independent events.

Given the generation rate λ of messages at a node, there are three sources of message loss: (i) dropping of arriving messaging due to the node buffer scheduling policy; (ii) collisions; (iii) reception errors. The mean rate of messages sent on air by a node is $1/\mathbb{E}[Y]$, i.e., the mean inter-departure rate. The net throughput in messages per unit time is therefore

$$\Theta = \frac{\gamma}{\mathbb{E}[Y]} = \frac{(1 - \tau)^{n-1} (1 - \text{PER})}{\mathbb{E}[X]/\tau + T_0 + \delta} \quad (16)$$

The normalized throughput is given by $\Theta_{\text{norm}} = \Theta/\lambda$. The throughput in bit/s can be obtained by considering the message payload L , i.e., it is $\Theta_{\text{bps}} = L\Theta$.

H. Access delay

The access time D is defined as the interval between the arrival time of a message that will be transmitted eventually and the completion of the transmission time of that message. Note that we disregard those messages that are overwritten by more recent ones.

At steady state, the probability of finding the queue in state 0 or 1 seen by an arrival that joins the queue is the same as the probability seen by a departing customer, hence $\mathcal{P}(\text{arrival finds an empty queue}) = \pi_0$.

The access time of a message that finds an empty queue amounts to $D = V + C$. If instead the message finds the queue already busy dealing with a previous message, it has to wait for a residual service time U , then the service time of the message can start. So, the access time is $D = U + C$. Summing up, we have

$$\varphi_D(s) = \varphi_C(s) [\pi_0 \varphi_V(s) + (1 - \pi_0) \varphi_U(s)] \quad (17)$$

There remains to evaluate the Laplace transform of the PDF of U , i.e., the time since the *last* arrival in a service time C and the end of that service time, given that at least one arrival occurs in the service time. The derivation is detailed in the Appendix, just replacing the random variables denoted there as X and V with C and U , respectively. The Laplace transform of the PDF of U is then found to be given by Equation (33), i.e., We have by Bayes theorem

$$\varphi_U(s) = \frac{\lambda}{s + \lambda} \frac{1 - \varphi_C(s + \lambda)}{1 - \varphi_C(\lambda)} \quad (18)$$

The mean access time is found as

$$\mathbb{E}[D] = \pi_0 (\mathbb{E}[V] + \mathbb{E}[C]) + (1 - \pi_0) (\mathbb{E}[U] + \mathbb{E}[C]) \quad (19)$$

I. Age of Information

The AoI is the age of messages received from other nodes at the tagged node. When a message is transmitted, it has already accumulated an age corresponding to its access time D . The AoI H is akin to the excess time in a renewal process. Its Cumulative Distribution Function (CDF), given $D = u$, is given by

$$\mathcal{P}(H \leq x | D = u) = \begin{cases} \int_0^{x-u} \frac{G_Z(t)}{\mathbb{E}[Z]} dt & x \geq u, \\ 0 & \text{otherwise.} \end{cases} \quad (20)$$

Here Z is the time between the reception of two consecutive *successful* messages from a given node. It is therefore the sum of consecutive inter-departure times, those elapsing between two consecutive transmissions of the tagged node that do not run into a collision or a packet reception failure. We have

$$Z = \sum_{i=1}^{\ell} Y_i^{(i)} \quad (21)$$

where $\mathcal{P}(\ell = k) = (1 - \gamma)^{k-1} \gamma$, $k \geq 1$ and γ is given in Equation (15). Note that D is independent of Z , with the assumption holding for our model. Removing the conditioning, we get

$$F_H(x) = \mathcal{P}(H \leq x) = \int_0^x f_D(u) du \int_0^{x-u} \frac{G_Z(t)}{\mathbb{E}[Z]} dt \quad (22)$$

The Laplace transform of the PDF of H is

$$\varphi_H(s) = \varphi_D(s) \frac{1 - \varphi_Z(s)}{s \mathbb{E}[Z]} \quad (23)$$

Since it is $\mathbb{E}[Z] = \mathbb{E}[Y]/\gamma$ and

$$\varphi_Z(s) = \frac{\gamma \varphi_Y(s)}{1 - (1 - \gamma) \varphi_Y(s)} \quad (24)$$

we have

$$\varphi_H(s) = \varphi_D(s) \frac{\gamma [1 - \varphi_Y(s)]}{s \mathbb{E}[Y] [1 - (1 - \gamma) \varphi_Y(s)]} \quad (25)$$

The mean AoI is calculated by deriving Equation (25) and setting $s = 0$:

$$\mathbb{E}[H] = \mathbb{E}[D] + \frac{\mathbb{E}[Y^2]}{2\mathbb{E}[Y]} + \mathbb{E}[Y] \left(\frac{1}{\gamma} - 1 \right) \quad (26)$$

We can find an asymptotic approximation of the Complementary Cumulative Distribution Function (CCDF) of the AoI. The dominant pole of the Laplace transform of the PDF of AoI is $-\zeta$, to be found as the smallest modulus root of the equation $\varphi_Y(-\zeta) = 1/(1 - \gamma)$. The CCDF of AoI can be approximated as a shifted exponential distribution, i.e.,

$$G_H(t) \approx \min\{1, a e^{-\zeta t}\} \quad (27)$$

The coefficient a can be found by imposing the mean value of this approximation be the same as the exact one, $\bar{H} = \mathbb{E}[H]$. Since the mean of a non-negative random variable with CDF given by $G(t)$ equals $\int_0^\infty G(t) dt$, it is easy to find that it must be $a = \exp(\zeta \bar{H} - 1)$. Then, we have

$$G_H(t) \approx \min\{1, e^{-\zeta(t - \bar{H}) - 1}\} \quad (28)$$

J. No queueing model of NoB policy

We can easily modify the analysis of the model described above to the case where no buffering is provided. Let us assume that as a new packet arrives at the MAC entity, the MAC layer does not accept new packets so long as it is engaged with that packet. As soon as the transmission of the current packet is over, the MAC layer entity is ready to accept new packets.

It is readily recognized that the analysis carried out in the previous sections can be cast onto this new model by simply setting $\pi_0 = 1$. Note that the master equation yielding the fixed point iteration for finding τ is then modified and hence values of τ are different in the two models.

Actually, the new model is simpler, since we do not need to keep track of the buffer status at the end of a transmission. The mean access time reduces to $D = V + C$ and the inter-departure time is simply $Y = R + C$.

Having no queueing avoids packets waiting in a buffer while the previous one goes through the access procedure and gets transmitted. On the other side, we miss the opportunity to have a packet ready as soon as the MAC layer entity is available again. Instead, we have to wait for a new packet to arrive. These facts lead to contrasting effects on the considered performance metrics, so that it is not obvious which system configuration is better. We will see that smaller AoI is achieved with no buffer provision, which leads to a simpler system design. More in depth, as λ tends to 0 (low message generation rate), it makes no difference whether a buffer is provided or not (which is pretty obvious in view of the fact that in that regime it is anyway $\pi_0 \sim 1$). For message generation rate around the optimal one and larger (moderate to large load regimes) the NoB policy achieves a smaller AoI, both as for the mean and of the tail of the PDF, as shown by numerical results.

IV. VALIDATION

A simulation model of the network has been implemented in MATLAB[®]. Physical layer parameters have been adjusted to represent IEEE 802.11bd for a high priority traffic category. The model accounts for all details of the access protocol, including post back-off and immediate transmission.

Post-back-off: When a message is transmitted and the node has an empty buffer, before going idle, it draws a back-off value and starts countdown. If no new message arrives within the countdown expiry, the node goes definitely back to idle state, waiting for new messages. Otherwise, the newly arrived message hijacks the on-going countdown.

Immediate transmission: When a node is idle and a new message is generated, the node checks if the channel is idle for an AIFS time. If that is the case, the frame containing the message is transmitted immediately, without any countdown. If instead the channel becomes busy before the AIFS time is completed, the node falls back to the usual access procedure.

Simulations were run for $n = 10$, a fixed packet size of $L = 500$ Byte, varying the mean message generation time $S = 1/\lambda$ between 1–100 ms. Air interface parameter

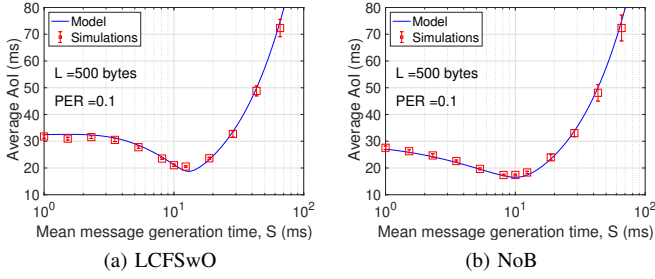


Figure 2. Average AoI as a function of the mean message generation time S .

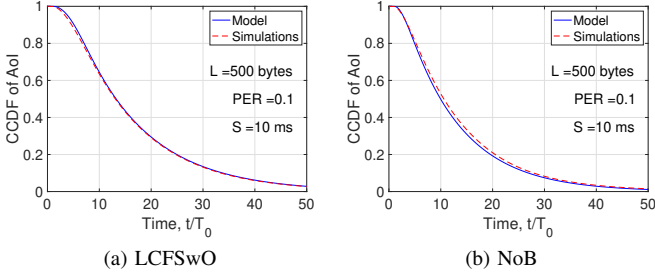


Figure 3. CCDF of the AoI for mean message generation time $S = 10$ ms.

and transmission times are consistent with IEEE 802.11bd amendment, as discussed in [18]. To evaluate the transmission time, we have assumed a robust modulation and coding scheme (MCS2, i.e., QPSK with code rate 1/2). We assume also a Packet Error Ratio (PER) of 0.1, i.e., reception of a message that does not run into a collision is deemed to be successful with probability 0.9. If a collision event occurs, reception is assumed to fail with probability 1. Simulations are displayed along with the 95-level confidence intervals.

Figure 2 illustrates the average AoI as a function of the generations time $1/\lambda$ for the LCFSwO (left plot) and NoB (right plot) policies. The model turns out to be accurate in both cases. As expected, there is an optimal value of the mean message generation time $S = 1/\lambda$ that minimizes the average AoI, trading off congestion of the channel (high levels of λ) with slackness of message generation (low levels of λ).

Figure 3 shows the CCDF of AoI for $S = 10$ ms. It can be noted that the model is accurate also with respect to probability distributions, besides matching average values. The accuracy

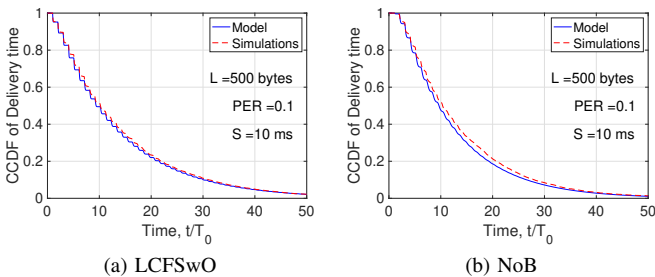


Figure 4. CCDF of the inter-departure times Y for mean message generation time $S = 10$ ms.

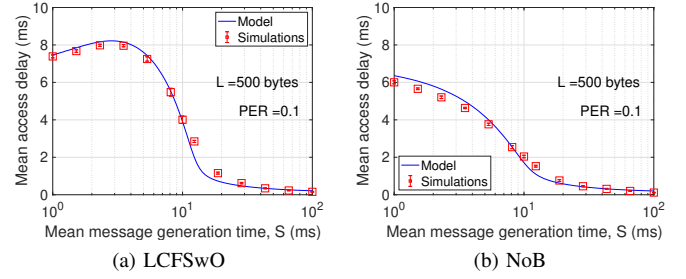


Figure 5. Mean access delay as a function of the mean message generation time S ($n = 10$ nodes)

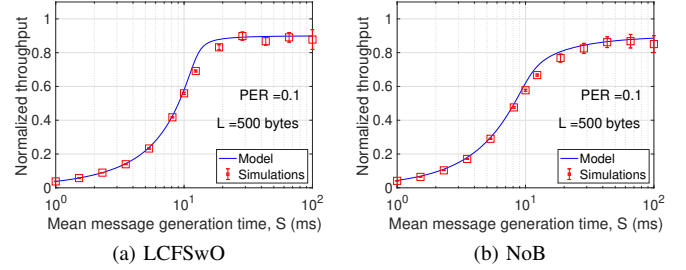


Figure 6. Average message throughput as a function of the mean message generation time S ($n = 10$ nodes)

of the model with respect to probability distributions is seen also in Figure 4, where the CCDF of the message delivery time Z (see Equation (21)) is plotted for the same value of the mean message generation time S as in Figure 3 and for $n = 10$ nodes.

Mean access time and normalized throughput are shown in Figures 5 and 6 respectively as a function of $S = 1/\lambda$, for $n = 10$ nodes. The mean access time in case of LCFSwO is higher than in case of NoB (not surprisingly) and exhibits a non-trivial behavior. It has a maximum for relatively high generation rate, then it drops sharply as the mean message generation time S is increased. In case no buffer is used, the mean access time decreases monotonically with S . As for the normalized throughput, it saturates to 90% (a percentage corresponding to the fraction $1 - \text{PER}$), as expected, for large S values. In that case the node is almost always idle when a new message arrives and the channel is lightly loaded, so that the collision probability is negligible. On the contrary, for high mean message generation rate λ , congestion of the channel and limited buffering induce high packet loss, thus making the throughput quite low. Notice that a high level of normalized throughput does not imply a low value of the average AoI.

V. COMPARISON OF LCFSwO AND NOB POLICIES

We use the model to investigate the impact of the scheduling policy at nodes on the AoI and throughput metrics, comparing the LCFSwO and NoB policies. This is done by varying:

- 1) The mean message generation time S between 1 ms and 100 ms.
- 2) The number n of nodes composing the network between 2 and 50.

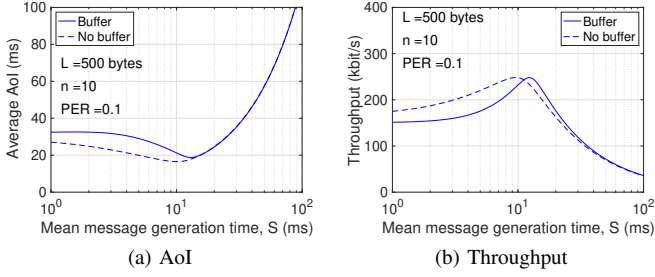


Figure 7. Average AoI and throughput as a function of the mean message generation time S ($n = 10$ nodes, $L = 500$ Byte)

3) The message payload length L between 100 Byte and 1500 Byte.

In all numerical examples we set $PER = 0.1$.

We evaluate the throughput (in kbit/s), the average AoI and the 90-quantile of AoI. The last one is evaluated by inverting numerically the Laplace transform of the PDF of AoI given in Equation (25). To this end, we use the Fourier series algorithm discussed in [19]. This algorithm turns out to be accurate and very efficient, giving the numerical inversion of the CDF on more than 600 points in less than 1 s of computation on a commercial PC, without any special software optimization.

In the next three figures solid lines refer to the LCFSwO policy, while dashed lines show performance of NoB policy.

Figure 7 shows the average AoI (left plot) and throughput (right plot) as a function of the mean message generation time S , for $n = 10$ nodes, $L = 500$ Byte. It is apparent that there are two distinct regimes. For low message generation time (high rate λ) congestion on the wireless channel dominates performance, hence collision is quite relevant. Having no buffering forces a node to wait for the next message, once the previous message has been transmitted. On the contrary, with LCFSwO, it is probable (the more, the smaller S) that a new message is ready as soon as the previous one has been transmitted. Hence nodes behave more aggressively and this apparently hurts AoI. Note that this result is not obvious a priori, given that providing a minimal buffering space avoids waiting for new message generation. While this is true, it appears that the adverse effect of increased collision probability dominates performance, resulting in the NoB policy to be superior. Not only is AoI smaller, but throughput as well turns out to be larger with no buffer (even though the achievable maximum throughput is almost the same, attained for different values of S in the LCFSwO and NoB cases). This means that the increased packet discarding due to lack of buffering space is outweighed by having less collisions in the NoB policy.

To look into message loss event in greater depth, Figure 8 shows the split of message flow according to the event affecting messages. The split is computed in fractions of the overall offered flow of messages. The plot on the left refers to the LCFSwO policy, the NoB policy being depicted in the plot on the right. The darkest area represents dropped messages. On top of that, the fraction of messages running into collision is shown with a less dark shade. A third fraction of messages

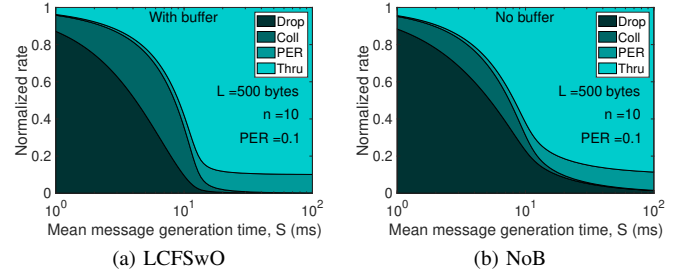


Figure 8. Split of offered message flow according to the event occurring to messages as a function of the mean message generation time S ($n = 10$ nodes, $L = 500$ Byte)

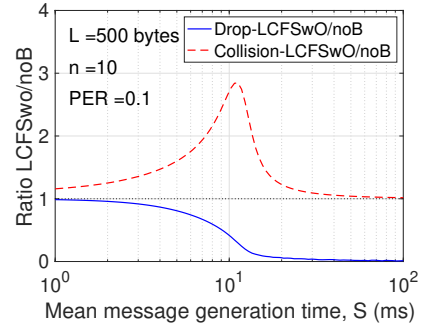


Figure 9. Ratio of the drop and collision probabilities of LCFSwO and NoB policies as a function of the mean message generation time S ($n = 10$ nodes, $L = 500$ Byte)

represents those that are transmitted without collision, but are detected with errors. The lightest part of the plot represent successfully delivered messages.

Comparing the two plots it appears that LCFSwO offers some advantage with respect to dropping, but it exhibits a much larger fraction of collided messages, especially in the low message generation time regime.

This phenomenon is made even more clear in Figure 9. It plots the ratio of the drop (solid line blue curve) and collision (dashed line red curve) probabilities of LCFSwO and NoB policies. In the left part of the figure (heavy traffic regime) the ratio of drop probabilities is close to 1, while on the right (low traffic regime) the ratio of the drop probabilities is much smaller than 1, i.e., LCFSwO has much better performance than NoB. However, under low traffic regime, the drop probabilities are both small and affect throughput and AoI only marginally. On the other hand, the ratio of collision probabilities of LCFSwO and NoB policies peaks at a quite large value (around 3) for intermediate values of the mean message generation rate S . It is apparent that NoB advantage lies in a substantial reduction of the collision probability, also when a sustained traffic is offered to the network, while only a marginal increase of the drop probability is suffered by offered messages in case of NoB with respect to LCFSwO. A different regime is visible for large message generation time S (low values of generation rate λ). In that case, collisions and packet drops are marginal and the two approaches end up with providing the same performance. However, large values of S imply a poor performance of

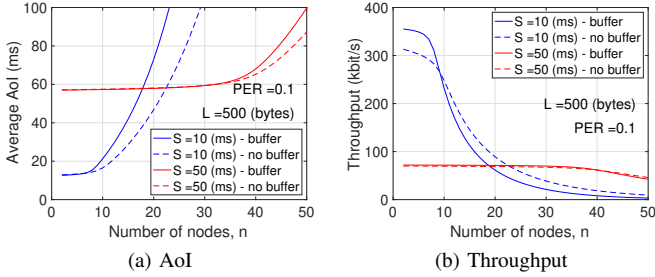


Figure 10. Average AoI and throughput as a function of the number of nodes n ($S = 10$ ms, $S = 50$ ms, $L = 500$ Byte)

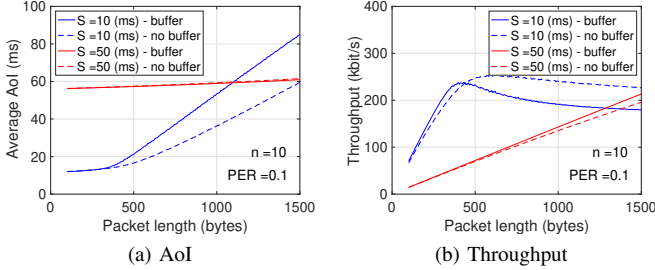


Figure 11. Average AoI and throughput as a function of message size L ($S = 10$ ms, $S = 50$ ms, $n = 10$ nodes)

average AoI and throughput.

Figure 10 shows the average AoI (left plot) and the throughput (right plot) as a function of the number of nodes n for mean message generation time $S = 10$ ms (blue curves) and $S = 50$ ms (red curves), with $L = 500$ Byte. In case a relatively large value of S is used (50 ms), both average AoI and throughput performance are weakly dependent on the number of nodes in the considered range. This value of S provides low throughput and average AoI of slightly less than 60 ms. Performance is substantially the same for the two scheduling policies. Much better performance is achieved for small n values in case $S = 10$ ms. However, when n grows and exceeds 10 nodes, performance degrades quickly. Moreover, NoB is superior with respect to the LCFSwO policy.

Figure 11 shows the average AoI (left plot) and the throughput (right plot) as a function of the message payload length L for mean message generation time $S = 10$ ms (blue curves) and $S = 50$ ms (red curves), with $n = 10$ nodes. It is confirmed that having no buffer provides better performance with respect to LCFSwO for $S = 10$ ms, while it is essentially indifferent which policy is adopted for $S = 50$ ms.

Increasing the message payload length, hence the transmission time, gives rise to a maximum for the throughput in case of $S = 10$ ms. This optimal regime corresponds to a best balance between amortizing overhead and packet discarding due to collision and packet drops. With the larger mean message generation time $S = 50$ ms, increasing the message payload length brings an improvements of throughput, given the low level of congestion of the wireless channel. However, both average AoI and throughput are quite worse than in case of $S = 10$ ms. Moreover, with low message generation rate, there

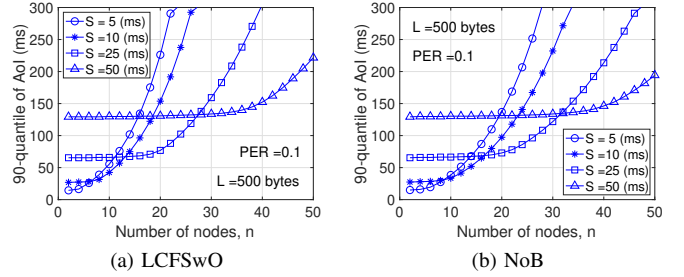


Figure 12. 90-quantile of the AoI as a function of the number of nodes for message length $L = 500$ Byte (left plot: one message queue; right plot: no queue).

is little difference between the two scheduling policies.

Finally, Figure 12 shows the 90-quantile of AoI as a function of the number of nodes n for LCFSwO (left plot) and NoB (right plot) policies, with $L = 500$ Byte and four values of S . The general behavior of the 90-quantile of AoI is similar to the average AoI: it has low and slowly increasing values for small network sizes. Then, as n grows, it ramps up with a fast growth rate. The knee of the curve is shifted towards smaller values of n in case of LCFSwO, again showing that better performance can be achieved by having no buffer.

The envelope of the considered curves suggests that S should be adapted as n changes, i.e., making it proportional to n . In fact, having large values of S is sub-optimal when the network is small, but proves to be far superior as the number of nodes grows. For low traffic regime (few nodes, high message generation time), a significant fraction of the AoI quantile value comes from the Poisson arrival assumption. Notice, however, that the randomness of Poisson arrivals adds to the MAC protocol random back-off in reducing collision probability.

VI. CONCLUSIONS

We have presented an analytical model for a CSMA-based network of agents exchanging one-hop update messages. The model yields probability distributions of all relevant quantities of message transfer, including access delay and AoI. Validation of the model against simulation shows that it exhibits high accuracy, while being computationally very efficient and stable.

We applied the model to gain insight into the role of buffering at MAC layer for update messages where freshness is the top requirement. While providing a minimum buffer for keeping the latest update while the node is busy sending the previous one seems to be a profitable strategy to improve throughput and freshness of delivered messages, it turns out that removing any buffer and simply letting the node wait for a new message, once it has completed its previous transmission, provides superior performance both in terms of throughput and AoI. The key reason of this result is that buffering makes nodes more “aggressive” and hence boosts collisions, unless the load on the wireless channel is under moderate to heavy traffic. Under light traffic regimes, providing buffering or not does not affect performance, as expected. This leads to simpler design of update message handling and also to simpler modeling and performance analysis.

Extensions of the model that we are pursuing are as follows: (i) accounting for variable transmission times, possibly with different PDFs in different classes of nodes; (ii) accounting for different message generation rates at the nodes; (iii) finding closed-form expressions for the message generation rate that minimizes AoI and maximizes channel effective utilization. A major extension of the model consists of relaxing the Poisson arrival process assumption. A pathway to this generalization consists of considering a slotted time axis, with slot time equal to the back-off slot time. This implies that transmission times are integer multiples of the back-off slot time. Then, we can define a modulating finite Markov chain with state $J(t) \in \{0, 1, \dots, J_{\max}\}$ at the beginning of slot t . We can define also the probabilities d_{ij}^0 and d_{ij}^1 of having no arrival or one arrival respectively and making a transition from state i to state j in the modulating Markov chain. This is an instance of Discrete-time Markov Arrival Process. The no-buffer scheme could then be analyzed by matrix-analytic methods.

REFERENCES

- [1] A. Vinel, L. Lan, and N. Lyamin, "Vehicle-to-vehicle communication in C-ACC/platooning scenarios," *IEEE Communications Magazine*, vol. 53, no. 8, pp. 192–197, 2015.
- [2] D. Orfanus, E. P. de Freitas, and F. Eliassen, "Self-Organization as a Supporting Paradigm for Military UAV Relay Networks," *IEEE Communications Letters*, vol. 20, no. 4, pp. 804–807, 2016.
- [3] J. Gielis and A. Prorok, "Improving 802.11p for Delivery of Safety-Critical Navigation Information in Robot-to-Robot Communication Networks," *IEEE Communications Magazine*, vol. 59, no. 1, pp. 16–21, 2021.
- [4] M. C. Lucas-Estañ, B. Coll-Perales, and J. Gozalvez, "Redundancy and Diversity in Wireless Networks to Support Mobile Industrial Applications in Industry 4.0," *IEEE Transactions on Industrial Informatics*, vol. 17, no. 1, pp. 311–320, 2021.
- [5] "IEEE Standard for Information Technology–Telecommunications and Information Exchange between Systems - Local and Metropolitan Area Networks–Specific Requirements - Part 11: Wireless LAN Medium Access Control (MAC) and Physical Layer (PHY) Specifications," *IEEE Std 802.11-2020 (Revision of IEEE Std 802.11-2016)*, pp. 1–4379, 2021.
- [6] G. Naik, B. Choudhury, and J.-M. Park, "IEEE 802.11bd and 5G NR V2X: Evolution of Radio Access Technologies for V2X Communications," *IEEE Access*, vol. 7, pp. 70 169–70 184, 2019.
- [7] G. Bianchi, "Performance analysis of the IEEE 802.11 distributed coordination function," *IEEE Journal on Selected Areas in Communications*, vol. 18, no. 3, pp. 535–547, 2000.
- [8] F. Cali, M. Conti, and E. Gregori, "Dynamic tuning of the IEEE 802.11 protocol to achieve a theoretical throughput limit," *IEEE/ACM Transactions on Networking*, vol. 8, no. 6, pp. 785–799, 2000.
- [9] D. Malone, K. Duffy, and D. Leith, "Modeling the 802.11 Distributed Coordination Function in Nonsaturated Heterogeneous Conditions," *IEEE/ACM Transactions on Networking*, vol. 15, no. 1, pp. 159–172, 2007.
- [10] X. Ma, J. Zhang, X. Yin, and K. S. Trivedi, "Design and Analysis of a Robust Broadcast Scheme for VANET Safety-Related Services," *IEEE Transactions on Vehicular Technology*, vol. 61, no. 1, pp. 46–61, 2012.
- [11] A. Kosta, N. Pappas, and V. Angelakis, "Age of Information: A New Concept, Metric, and Tool," *Foundations and Trends® in Networking*, vol. 12, no. 3, pp. 162–259, 2017.
- [12] A. Maatouk, M. Assaad, and A. Ephremides, "On the Age of Information in a CSMA Environment," *IEEE/ACM Transactions on Networking*, vol. 28, no. 2, pp. 818–831, 2020.
- [13] A. Baiocchi, I. Turcanu, N. Lyamin, K. Sjöberg, and A. Vinel, "Age of Information in IEEE 802.11p," in *17th IFIP/IEEE International Symposium on Integrated Network Management (IM): ITAVT Workshop*, Virtual Conference: IEEE, May 2021.
- [14] A. Baiocchi and I. Turcanu, "Age of Information of One-Hop Broadcast Communications in a CSMA Network," *IEEE Communications Letters*, vol. 25, no. 1, pp. 294–298, 2021.

- [15] M. van Eenennaam, L. Hendriks, G. Karagiannis, and G. Heijnen, "Oldest packet drop (OPD): A buffering mechanism for beaconing in IEEE 802.11p VANETs (poster)," in *2011 IEEE Vehicular Networking Conference (VNC)*, 2011, pp. 252–259.
- [16] T. Li, D. Leith, and D. Malone, "Buffer Sizing for 802.11-Based Networks," *IEEE/ACM Transactions on Networking*, vol. 19, no. 1, pp. 156–169, 2011.
- [17] L. Hendriks, "Effects of transmission queue size, buffer and scheduling mechanisms on the IEEE 802.11p beaconing performance," in *15th Twente Student Conference, University of Twente, Faculty of Electrical Engineering, Mathematics and Computer Science*, 2011.
- [18] W. Anwar, N. Franchi, and G. Fettweis, "Physical Layer Evaluation of V2X Communications Technologies: 5G NR-V2X, LTE-V2X, IEEE 802.11bd, and IEEE 802.11p," in *2019 IEEE 90th Vehicular Technology Conference (VTC2019-Fall)*, 2019, pp. 1–7.
- [19] J. Abate and W. Whitt, "Numerical inversion of Laplace transforms of probability distributions," *ORSA Journal on computing*, vol. 7, no. 1, pp. 36–43, 1995.

APPENDIX

Let X denote a positive random variable. Let V be the time elapsing since the *last* arrival of a Poisson process with mean rate λ , occurring within X , and the end of the time interval X .

Let X' denote the time interval X conditional on at least one arrival. We have

$$\begin{aligned} \mathcal{P}(X' > x) &= \mathcal{P}(X > x | A(0, X) > 0) \\ &= \frac{\int_x^\infty (1 - e^{-\lambda u}) f_X(u) du}{\int_0^\infty (1 - e^{-\lambda u}) f_X(u) du} \\ &= \frac{\int_x^\infty (1 - e^{-\lambda u}) f_X(u) du}{1 - \varphi_X(\lambda)} \end{aligned}$$

where $A(u, v)$ is the number of arrivals in the time interval $[u, v]$ according to the Poisson process with mean rate λ . Taking the derivative, we obtain the PDF of X' :

$$f_{X'}(x) = \frac{(1 - e^{-\lambda x}) f_X(x)}{1 - \varphi_X(\lambda)} \quad (29)$$

We are now ready to derive the probability distribution of V :

$$\mathcal{P}(V > t) = \int_t^\infty \mathcal{P}(V > t | X' = x) f_{X'}(x) dx \quad (30)$$

Let $P(t|x) = \mathcal{P}(V > t | X' = x)$ denote the conditional probability inside the integral. It can be evaluated as follows.

$$\begin{aligned} P(t|x) &= \frac{\mathcal{P}(A(0, x-t) > 0, A(x-t, x) = 0)}{\mathcal{P}(A(0, x) > 0)} \\ &= \frac{(1 - e^{-\lambda(x-t)}) e^{-\lambda t}}{1 - e^{-\lambda x}} = \frac{e^{-\lambda t} - e^{-\lambda x}}{1 - e^{-\lambda x}} \end{aligned}$$

Substituting the expression of the PDF of X' and the result above into Equation (30), we get:

$$\mathcal{P}(V > t) = \int_t^\infty (e^{-\lambda t} - e^{-\lambda x}) \frac{f_X(x)}{1 - \varphi_X(\lambda)} dx \quad (31)$$

Taking the derivative, we finally find the PDF of V :

$$f_V(t) = \frac{\lambda e^{-\lambda t} \mathcal{P}(X > t)}{1 - \varphi_X(\lambda)} \quad (32)$$

The corresponding Laplace transform is

$$\varphi_V(s) = \frac{\lambda}{1 - \varphi_X(\lambda)} \frac{1 - \varphi_X(s + \lambda)}{s + \lambda} \quad (33)$$